SSRG International Journal of Electrical and Electronics Engineering
ISSN: 2348-8379/ https://doi.org/10.14445/23488379/IJEEE-V11I11P136

Volume 11 Issue 11, 381-398, November 2024

Original Article

Efficient Load Demand Prediction in Complex Energy Systems Using Modified Optimization Algorithms

I.J. Jithin Kumar[1], S. Divyapriya[2]

[1,2]*Department of Electrical Engineering, Karpagam Academy of Higher Education, Tamilnadu, India.*

[1]*Corresponding Author : JithinKumar.I.J@outlook.com*

Received: 20 September 2024 Revised: 21 October 2024 Accepted: 19 November 2024 Published: 30 November 2024

Abstract - *Accurate load forecasting is essential for effective energy management, especially in regions with dynamic energy consumption patterns. While Support Vector Regression (SVR) is widely used for load forecasting, its performance degrades on large datasets due to computational constraints in kernel learning. To overcome this difficulty, this study suggests combining SVR with the Particle Swarm Optimization (PSO) and Modified Harris Hawk's Optimization (MHHO) algorithms to develop two hybrid SVR models, SVR-PSO and SVR-MHHO. Results demonstrate that both SVR-MHHO and SVR-PSO outperform traditional SVR, with SVR-MHHO exhibiting superior performance. Leveraging MATLAB/Simulink-2021a®, a modified form of the HHO algorithm is developed to improve search efficiency. Specifically, SVR-MHHO achieved the highest R^2 values (0.9932, 0.8896, 0.9921, and 0.9287), lowest MSE values (0.0004, 0.0062, 0.0005, and 0.0078), and lowest MAPE values (0.1479, 0.1323, 0.0768, and 0.1896) across the cities of Delhi, Mumbai, Kolkata, and Bangalore, respectively. Additionally, SVR-MHHO demonstrated advantages over SVR-PSO for load demand prediction in all cities. This study highlights the efficacy of hybrid SVR algorithms and their potential for improving load forecasting accuracy in energy management applications.*

Keywords - *PV panel, Microgrid, BESS, Peak load shaving, State of charge.*

1. Introduction

In addition to the rapid advancement of civilization, the world's population and economy are growing, implying that the need for power consumption will likely expand soon [1]. Furthermore, as society develops and the population grows significantly, there is an increased need for power, immediately impacting the need for more electricity. Energy management addresses the three main issues of distribution, transmission, and power production. With the rapid population and economic expansion, residential buildings' power consumption has expanded dramatically.

Electricity is a vital and increasingly crucial energy source in modern life, with its importance continually growing [2]. Its clean and efficient nature makes it a focal point of research endeavors [3]. Unlike material products, electricity cannot be stored in large quantities, necessitating generation on-demand. The complexity of electricity demand patterns, compounded by market deregulation, poses challenges in accurate forecasting and the risk of financial loss.

Anticipated growth in global electricity demand, driven by population expansion, rising living standards, and technological advancements, underscores the need for proactive load prediction to manage power systems effectively. Forecasting electricity needs in advance is imperative to inform generation decisions, especially amidst the proliferation of high-power appliances, smart grids, electric vehicles, and renewable energy technologies [4].

Load Forecasting (LF) is significant in the electricity industry's planning and operational domains. LF garners significant attention due to its necessity across various applications. It directly impacts national security, societal functioning, and economic development [5]. It entails projecting the energy needed to meet consumer demands, essential for stable economic conditions and dependable power system performance. Accurate electric load forecasting facilitates important decision-making procedures, including infrastructure management, load switching, and the generation and purchase of electricity. Giving insights into future consumption and load needs facilitates proactive planning for energy upgrades and helps avoid circumstances with too little or too much power generated.

The precision of load forecasting is paramount for efficiently scheduling energy generation capacity and managing power systems. Accurate forecasts yield substantial cost savings in operations and maintenance, besides aiding in informed decision-making for future infrastructure development [6]. Also, load forecasting is foundational in designing forthcoming generation, transmission, and

distribution facilities. Nevertheless, achieving the desired accuracy in electric LF frequently proves challenging due to the influence of various unpredictable factors like economic fluctuations, societal activities, governmental policies, and climate variability. The assessment of electricity demand involves the periodic accumulation of use, with consideration given to hourly, daily, weekly, monthly, and annual intervals. Figure 1 illustrates the classification of the LF according to the length of the planning horizon [7].

These models are essential for efficient power system planning, financial management, and electric sales. LF can be subdivided into energy and demand forecasts based on the horizon. Demand forecasting estimates future customer demands and predicted load growth rates, which helps evaluate resource requirements for production, transmission, and distribution systems [8]. Conversely, energy forecasting helps determine future fuel requirements and the facilities that will be required [9].

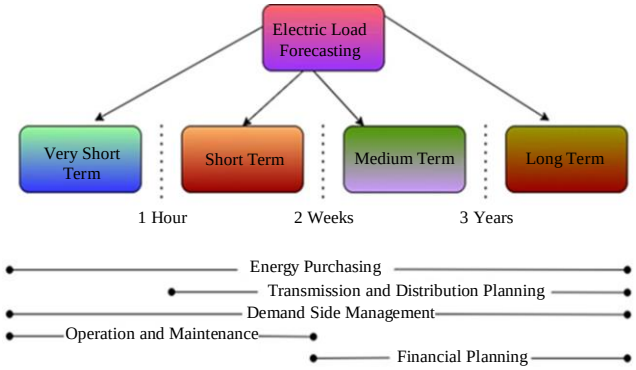

Fig. 1 Categories of forecasting loads according to forecasting horizons

Supply and demand balancing depends on load forecasting. However, several intricate aspects make load forecasting difficult. Previous load patterns, demographic information, and weather influence the efficiency of forecasts. The appropriate frameworks must be chosen after data analysis and geographical and equipment variables are considered. Although it presents difficulties, accurate forecasting is advantageous to utility firms; nonetheless, errors can result in losses. In order to tackle this, a unique method called MHHO-SVR is put forth in the proposed study, which attempts to increase load forecasting efficacy and reduce errors. The following are the main contributions of the suggested study:

- To Integrate Modified Harris Hawk's Optimization (MHHO) and PSO with SVR for load forecasting.
- To demonstrate the superior performance of SVR-MHHO and SVR-PSO over conventional SVR models.

The remaining sections of the paper are structured as follows. The following section briefly discusses the most popular load forecasting models and techniques in the literature. The methodology employed in this study is carried out in Section 3. The research results and findings are examined and assessed in Section 4. Ultimately, the study's conclusions are provided in Section 5.

2. Related Works

Tarmanini et al. (2023) [10] discussed how smart grid technologies require precise electricity demand forecasting. They used MAPE to compare the Auto Regressive Integrated Moving Average (ARIMA) and Artificial Neural Network (ANN) approaches for load prediction. Applying daily power data for eighteen months to 709 Irish households, ANN provided better results for non-linear load data than ARIMA. Model evaluation and forecasting efficiency demonstration were conducted using 〖MATLAB〗^TM. Nevertheless, the study's ability to precisely forecast peak consumption was limited. ANN performed better than ARIMA, but it was less accurate in predicting peak consumption.

Mohammed et al. (2022) [11] investigated how a lack of sufficient training data and accumulation of errors made it difficult for conventional ANNs to predict long-term electrical load demand. To solve these problems, they created the Adaptive Backpropagation Algorithm (ABPA), which incorporates adjustment parameters to reduce behavioral differences between datasets that are trained and those that are not. Using real monthly consumption data from 2011 to 2020, their computational analysis demonstrated the superiority of ABPA, yielding minimal MAPE and MSE values of 0.045 and 1.195.650, respectively. Although ABPA works well, its applicability to highly stationary datasets is limited because of the significant behavioral variations between training and validation datasets necessary for effective implementation.

In order to improve power systems' performance, Ahmed (2022) [12] underlined the growing need for precise electric load demand forecasting. An important aspect of smart grid operations is Short-Term Load Forecasting (STLF), which has led to the investigating of different Al-based methods. A DNN model with feature selection was presented in this work, and leaky ReLU showed better accuracy. The model was validated across scenarios of load demand and seasons by utilizing evaluation criteria such as MAPE and MSE. Notably, hybrid models that combined RNN with ANN and LSTM fared better in one-day forecasts; RNN's MAPE accuracy was 1.01%. Nevertheless, there are certain drawbacks, such as the requirement for more studies on the effectiveness of feature descriptors and the possibility of biased data being lost during dimension reduction methods.

Three approaches were used in Alotaibi's study (2022) [13] to estimate STLF: Decision Tree (DT) based prediction, multilayer perceptron-based ANN, and Deep Neural Network (DNN). Aiming to increase predicting accuracy, new

predictive variables were added. Outperforming other models statistically, the DNN model performed better. They analyzed data from Canadian Climate Data and the Independent Electricity System Operator. Limitations of the study include the omission of qualitative components and reliance on numerical data, notwithstanding its merits. Hybrid models and ensemble techniques were also not explored.

By contrasting several machine learning techniques, Rao et al. (2022) [14] addressed the difficulty of LF in cluster microgrids. Methods including support vector machines, ANN, linear regression, and long short-term memory were assessed. Despite having higher computing needs, the results showed that ANN performed better than the others in terms of RMSE, MAPE, MSE, and MAE. For ANN training, optimization techniques like Levenberg-Marquardt were investigated; the former demonstrated good performance in testing, training, and error analysis. Nevertheless, several drawbacks were mentioned, including possible overfitting and computational complexity.

Machado et al. (2021) [15] suggested employing a Feed-Forward Neural Network (FFNN) to enhance load demand estimates and integrate error correction through the use of another FFNN. The outcomes showed that the forecast quality was better than the benchmark models. They used medium voltage grid data from an industrial sector, recorded every 10 minutes between October 1, 2016, and March 31, 2017. On the other hand, the accuracy of longer-term forecasts declined, suggesting a higher degree of data uncertainty. The suggested methodology greatly increased forecast accuracy over a range of time horizons, but execution time is affected by its complexity. Some limitations include evaluating generalizability on larger datasets with various consumer profiles and making any necessary adjustments for various consumer types.

Jalali et al. (2021) [16] used Convolutional Neural Networks (CNNs) optimized using Enhanced Grey Wolf Optimizer (EGWO) to tackle the complexity of electrical LF. Compared to benchmark methods, their EGWO- CNN method reduced optimization, training, and testing times by automating CNN hyperparameters. When EGWO-CNN was evaluated using data from the Australian Energy Market Operator, it showed decreased RMSE, MAE, and MAPE and better predicting accuracy. Nevertheless, drawbacks include the possibility of overfitting brought on by CNN architectures' intricacy and their dependence on historical data, which make it more difficult to adjust to unforeseen variations in load patterns.

In order to ensure worldwide forecasting without affecting data privacy, Moradzadeh et al. (2021) [17] presented a unique technique for heating load demand forecasting in buildings: Cyber-Secure Federated Deep Learning (CSFDL). The strategy entailed using edge computing to protect data confidentiality while educating a global server with data from seven customers. The results showed high accuracy with a correlation coefficient of 99.00% on familiar data and 98.00%, 93.00%, and 70.00% on out-of-sample data. The better performance of CSFDL was demonstrated through comparison with traditional methods, particularly for customers lacking training data. Limitations include difficulties adapting the model to dynamic building contexts and scalability issues with growing client numbers.

The need for precise STLF in power plant design was highlighted by Rafi et al. (2021) [18]. They suggested using historical load, meteorological, and holiday data to create Machine Learning (ML) models for 168-hour projections. Extreme Gradient Boosting Regressor (XGBoost) fared better than other examined models, improving interpretability. With data that was made accessible to the public between January 2015 and June 2020, XGBoost continuously raised MAPE and RMSE. However, RF displayed erratic spikes, and MLR and KNN had problems predicting holidays. One of the model's drawbacks is its dependence on past data, which makes regular model modifications necessary to accommodate changing consumption trends.

The importance of precise load demand forecasting in smart grid and building contexts was highlighted by Lulu Wen et al. (2020) [19]. They suggested a deep learning model that considers the complexity and variability of residential energy demand forecasts. The model outperformed standard methods in terms of accuracy, using hourly-measured data from Austin, Texas, USA. They achieved great accuracy and provided the possibility of imputation for missing data by utilizing a DRNN-GRU architecture to capture time dependencies in load data. It was acknowledged that there were several limits, such as the model's reliance on weather data from the future and the requirement for deeper networks and finer-grained data for improved performance.

To handle the complexity of electric load profiles, a hybrid STLF approach was proposed by Hafeez et al. (2020) [20]. The model used a Factored Conditional Restricted Boltzmann Machine (FCRBM) for training and prediction, Modified Mutual Information (MMI) for feature selection and data pre-processing, and Genetic Wind-Driven Optimization (GWDO) for optimization.

The suggested technique performed better than benchmark models when tested using historical data from three power grids in the United States. It increased forecast accuracy by 31.2% over MI-ANN, 17.3% over Bi-level, and 4.7% over AFC-ANN. Nevertheless, drawbacks include the requirement for substantial parameter adjustment and the possibility of overfitting due to deep learning approaches. Furthermore, real-time applications encounter difficulties due to the computational resource requirements.

Despite significant advancements in load demand forecasting methodologies, substantial research gaps persist, particularly in addressing the limitations of managing intricate nonlinear interactions and sudden anomalies in time series data. Existing models often struggle with the computational intensity required for real-time applications, hindering their scalability and practical implementation. Additionally, integrating external variables remains a challenge, as many frameworks exhibit difficulties adapting to inconsistent datasets and dynamic environmental conditions. This situation underscores the necessity for developing innovative algorithms that can efficiently handle high-dimensional feature spaces while maintaining robustness against outliers and irregular patterns. Furthermore, exploring hybrid architectures that seamlessly blend ensemble techniques and recurrent neural networks may provide a pathway to enhance predictive accuracy without incurring excessive computational overhead. Ultimately, the quest for more efficient data acquisition and processing methods is critical, as current practices often fall short of meeting the demands of contemporary energy systems.

3. Materials and Methods

Support Vector Regression (SVR) and Modified Harris Hawks Optimization (MHHO) are used in this study to present an innovative method for STLF in faraway regions, including Delhi, Mumbai, Kolkata, and Bangalore. This hybrid approach seeks to enable more efficient energy management in isolated places by improving forecasting accuracy in regions with distinct data features. Figure 2 depicts the general steps involved in developing the proposed model.

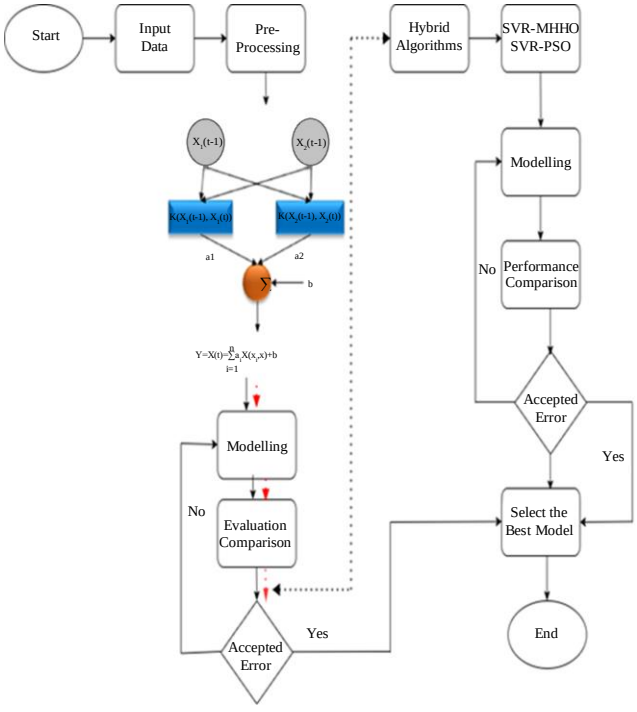

Fig. 2 Flowchart of the proposed study

The issue of identifying the most efficient technique in real-world applications is the reason for using several optimization algorithms for models. Choosing the most accurate method is difficult because there are many evaluation criteria and different input combinations. To enhance the accuracy and speed of the framework, data collection, preprocessing, and normalization were carried out in accordance with Equation (1). Improving the predictive model's efficacy requires this preprocessing step. Various statistical measures are employed to analyze the performance of Al-based and regression models objectively. The holdout approach, similar to a condensed version of the k-fold method, separates data into training and testing sets at random to maintain independence for effective model optimization.

$$y = 0.05 + (0.95) * \left(\frac{x - x_{min}}{x_{max} - x_{min}}\right) \quad (1)$$

Where x is the data being measured, y is the normalized data, and x_{max} and x_{min} are the measured data's maximum and minimum values correspondingly. Equation (2) presents the model combination.

$$f\begin{cases} Load\ Demand\ (W) = \\ M_1 = (Temperature) \\ M_2 = (Temperature + wind) \\ M_3 = (Temperature + wind + solar\ radiation) \end{cases} \quad (2)$$

3.1. Data Collection and Pre-Processing

The proposed study entailed collecting load demand data from remote places in Indian cities. Because of the inherent difficulty in assuring the reliability and comprehensiveness of the data sourced from these varied regions, the gathering phase of this dataset requires thorough attention to detail. A wide range of resources, such as local power companies, state governments, and pertinent academic organizations, were used to retrieve load demand data from the past over an extended period. Demographic and environmental aspects were also considered to appropriately contextualize the load demand data. The gathered data was put through stringent quality checks and preparation procedures to eliminate anomalies, fix inconsistencies, and standardize formats to guarantee authenticity and robustness. The entire dataset was then split into two subsets: a calibration set used to train and develop the model (70%) and a verification set (30%) used to assess the model's efficiency.

3.2. Support Vector Regression

SVR is a variant of the Support Vector Machine (SVM) technique designed for regression tasks, especially when there is a nonlinear relationship between the target and input variables [21]. It is based on selecting a hyperplane that maximizes the margin and fits the data best while allowing for deviations from the hyperplane a feature known as the epsilon-insensitive tube. To divide the training data into two classes those inside the epsilon-insensitive tube and those outside a

hyperplane in a high-dimensional space is defined as part of the SVR design. Equation (3) provides a mathematical representation of the SVR model.

$$y = f(X) = \omega.\varphi(X) + b \tag{3}$$

Where ω is the weighting vector, $\varphi(X)$ indicates the mapping function employed in the feature space, and b is a constant factor or bias. The main aim of SVR is to find the optimal values of ω and b that minimize the empirical risk, subject to a margin of tolerance for deviations. The minimization problem, as stated by Equation (4) to (7), estimates the coefficients of ω and b.

$$Minimize: \ 0.5\omega^2 + c\frac{1}{N}\sum_{i=1}^{N}(\xi_i + \xi_i^*) \tag{4}$$

$$y_i - (\omega, x_i + b) \geq \varepsilon + \xi_i \tag{5}$$

Subject to:

$$(\omega, x_i + b) - y_i \geq \varepsilon + \xi_i^* \tag{6}$$

$$\xi_i, \xi_i^* \geq 0 \tag{7}$$

The parameters of the model are ε and c. As seen in Figure 3, the function's smoothness is measured by the term $0.5\omega^2$, and the trade-off between smoothness and empirical risk is assessed by the term c. Furthermore, in the ε -tube model of function approximation, ξ_i, ξ_i^* are the positive slack variables that quantify the difference between real and matching border values.

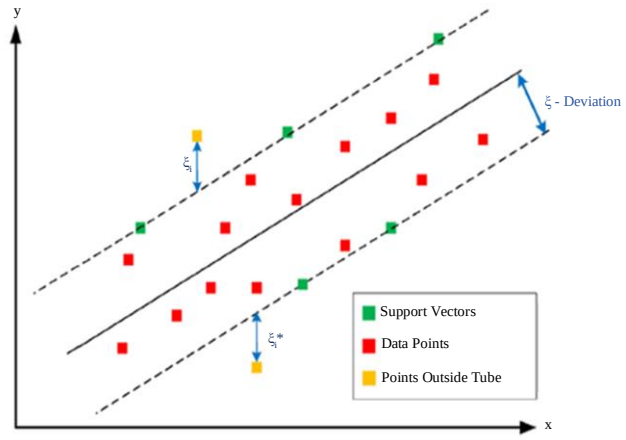

Fig. 3 Linear regression in the SVR algorithm with an epsilon-intensive band

The solution for the non-linear regression function is achieved by using the Lagrangian functions, as indicated in Equation (8).

$$f(X) = \sum_{i=1}^{N}(\alpha_i - \alpha_i^*)K(X_i, X_j) + b \tag{8}$$

Where $K(X_i, X_j)$ is the kernel function that displays the inner product of X_i and X_j in D-dimensional feature space, and α_i, α_i^* are Lagrangian multipliers. The Radial Basis Functions (RBF) kernel, specified by Equation (9), was used in this study [22].

$$K(X_i - X_j) = exp\left(-\gamma\|X_j - X_i\|^2\right) \tag{9}$$

Where the kernel parameter is denoted by γ. X_i and X_j represent the inputs in the i^{th} and j^{th} dimensions, respectively.

3.3. Particle Swarm Optimization

Kennedy and Eberhart developed Particle Swarm Optimization (PSO), a computational optimization approach based on the social behavior of flocks of birds and schools of fish [23]. PSO defines the population as a "swarm" and the individuals as "particles." N particles make up the swarm X, which is located in an m-dimensional search space.

Each particle possesses two vectors: the swarm velocity, represented as $v_i = (v_{i1,}v_{i2},\ldots,v_{im})$, and the swarm position, represented as $x_i = (x_{i1,}x_{i2},\ldots,x_{im})$. Every particle is accelerated while seeking the particles, as shown in Figure 4, at the local best $(i.e, p_i^{best}(k)\ of\ i^{th}\ swarm\ at\ iteration\ k)$ and globally best $(i.e, G_k^{best}\ at\ iteration\ k)$ positions.

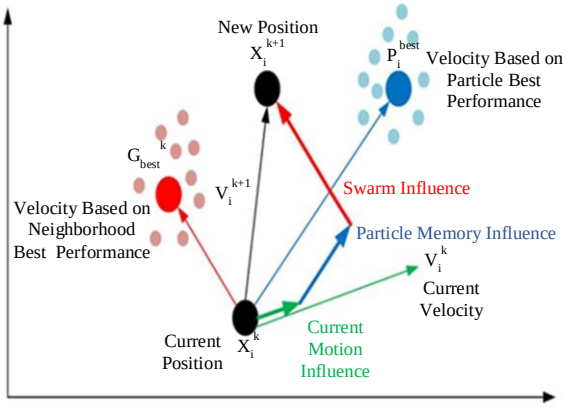

Fig. 4 Conceptual updates of a searching point's location and speed via PSO

The locally optimal position is considered to be P_i^{best}Whereas the globally optimal position is considered to be G_{best}. Every particle updates its location and velocity during the iterative mechanism. With Equation (10) and (11), respectively, the position and velocity of every particle $(i.e, i = 1,2,\ldots,N)$ are updated. This process continues iteratively until a stopping condition is satisfied, including attaining the maximum number of iterations or arriving at a satisfactory outcome.

$$\left(V_i(k+1)\right) = w \times V_i(k) + c_1 \times r_1 \times \left(p_i^{best}(k) - x_i(k)\right) + c_2 \times r_2 \times \left(G_{best}(k) - x_i(k)\right) \quad (10)$$

$$x_i(k+1) = x_i(k) + V_i(k+1) \quad (11)$$

Where w is the inertia weight; a greater w aids the global search, while a smaller w enables the local search. This allows for a balance between local and global explorations. N is the overall count of particles, r_1 and r_2 are random values in the range of $(0,1)$, c_1 and c_2 are acceleration positive numbers, and parameter k is the count of iterations.

3.4. Harris Hawks Optimization

The HHO swarm intelligence optimization technique, which has a strong global search capability and only modifies a few parameters, was developed by Heidari et al. [24] in 2019 and is designed to resemble the way Harris eagles locate and pursue prey in nature. The Harris hawk, renowned for its cunningness and strength, has exceptional cooperative hunting abilities in bringing down its victim. In this illustration, the hawk population stands for a group trying to grab a rabbit. The hawks attempt to apprehend the elusive prey by utilizing seven techniques or a surprise pounce, as shown in Figure 5.

(a) Harris Hawks (b) Surprise Pounce

Fig. 5 The actions of Harris's hawk

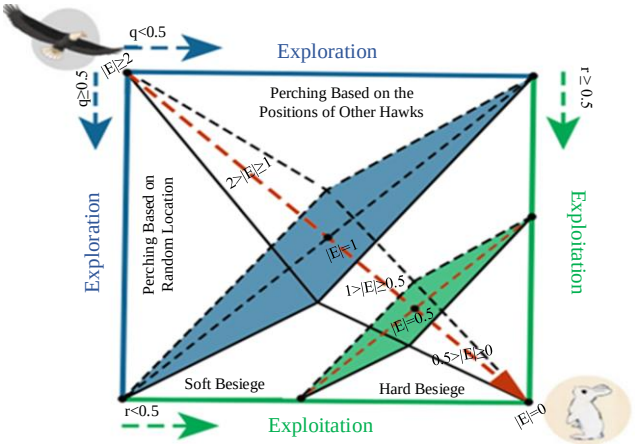

Fig. 6 Different HHO phases

The group uses other strategies to guarantee success if the lead hawk cannot pursue its victim because of its agile movements. The hawks can successfully follow and exhaust their prey until it is caught because of their cooperative approach. The seized prey is the optimal/global solution in the HHO algorithm, while the hawks represent potential solutions. The foraging process comprises three primary phases: exploration, transition from exploration to exploitation, and exploitation, as shown in Figure 6.

3.4.1. Exploration Phase

A rabbit might represent the prey Harris hawks seek during the exploratory period. Equation (12) explains Harris hawks' two techniques to keep their locations updated when they use their excellent vision to discover and track rabbits.

$$X_i(t+1) = \begin{cases} X_{rand}(t) - r_1 \left| X_{rand}(t) - 2r_2 X_i(t) \right|, & q \geq 0.5 \\ \left(X_{rabbit}(t) - X_m(t)\right) - r_3\left(LB + r_4(UB - LB)\right), & q < 0.5 \end{cases} \quad (12)$$

Where the positions of the rabbit and the i^{th} hawk at iteration t are represented by $X_i(t)$ and X_{rabbit}, respectively. The positions of the randomly chosen hawk are denoted by $X_{rand}(t)$, the i^{th} hawk at the next $(t+1)^{th}$ iteration is denoted by $X_i(t+1)$, four random numbers between $[0,1]$ are r_1, r_2, r_3, and r_4; q is the random number spans between $[0,1]$ that is used to switch the strategy; and $X_m(t)$ is the mean position of the current population as per Equation (13), where $[LB, UB]$ indicates the search space and N_p is the population size.

$$X_m(t) = \frac{1}{N_p}\sum_{i=1}^{N_p} X_i(t) \quad (13)$$

3.4.2. Transition from Exploration to Exploitation

The primary factor influencing the transition of Harris hawks from their global chase (exploration) to their targeted local chase (exploitation) is the prey's (rabbit's) escape energy E, which can be computed using Equation (14).

$$E = 2E_0\left(1 - \frac{t}{T}\right) \quad (14)$$

Where T denotes the maximum number of iterations and E_0 is the random variable between $(-1,1)$ in each iteration. As a result, the escaping energy E is between -2 and 2. The rabbit may be able to escape when $|E| \geq 1$, in which case the Harris hawks launch an extensive search (exploration). When $|E| < 1$, the rabbit is considered weak, and the Harris hawks conduct a local search or exploration.

3.4.3. Exploitation Phase

Harris hawks are known to besiege rabbits upon spotting them and await an opportunity to strike. But, during a siege, the rabbit might manage to break free. Thus, Harris hawks must constantly modify their flying plans to account for the rabbit's unpredictable behavior. The exploitation phase will employ four tactics to simulate the hunting behavior of a

Harris hawk, which will be switched by the escaping energy E and a random r as follows [25]:

Soft Besiege

The rabbit has enough energy to try to break free from the siege by jumping whenever it desires, but it is eventually unable to do so. Harris hawks can take advantage of this by surrounding the rabbit and making a surprise pounce. This occurs when |E|≥0.5 and r≥0.5. Equations (15)-(17) are used to create this strategy.

$$X(t+1) = \Delta X(t) - E|JX_{rabbit}(t) - X(t)| \quad (15)$$

$$\Delta X(t) = X_{rabbit}(t) - X(t) \quad (16)$$

$$J = 2(1 - r_5) \quad (17)$$

Where J is the rabbit's random jump strength, r_5 is the random value in a range of 0 and 1, and $\Delta X(t)$ is the difference between the optimum individual and the current individual.

Hard Besiege

The rabbit is tired and lacks the energy or chance to escape when |E|<0.5 and r≥0.5. This allows the Harris hawks to sneak up on the rabbit by encircling it and launching a surprise pounce. Equation (18) is used to create this strategy.

$$X(t+1) = \left|X_{rabbit}(t) - E|\Delta X(t)|\right| \quad (18)$$

Soft Besiege with Progressive Rapid Dives

The rabbit has enough energy to break free from its encirclement when |E|≥0.5 and r<0.5. Therefore, the Harris hawks must encircle the rabbit more cleverly before making a surprise pounce. The two approaches used by Harris Hawks to encircle the rabbit are as follows: if the first approach fails, the second one is utilized.

The first approach is

$$Y = X_{rabbit}(t) - E|JX_{rabbit}(t) - X(t)| \quad (19)$$

The second approach is

$$Z = Y + S * LF(D) \quad (20)$$

Where D is the search space's dimension, $LF(\cdot)$ is the Levy flight function as determined by Equation (21), and S is a random vector of $1 \times D$ dimensions.

$$LF(x) = 0.01 * \frac{\mu * \sigma}{\frac{1}{|\nu|^{\frac{1}{\beta}}}}, \sigma = \left(\frac{\Gamma\left(1+\beta * \sin\frac{\Pi\beta}{2}\right)}{\Gamma\left(\frac{1+\beta}{2}\right) * \beta * 2^{\left(\frac{\beta-1}{2}\right)}} \right)^{\frac{1}{\beta}} \quad (21)$$

Where μ and ν are random values in the range of 0 and 1, and β is a constant customized to 1.5. Consequently, Equation (22) can be used to model the updating method for this phase.

$$X(t+1) = \begin{cases} Y, F(Y) < F\left(X(t)\right) \\ Z, F(Z) < F\left(X(t)\right) \end{cases} \quad (22)$$

Hard Besiege with Progressive Rapid Dives

The rabbit may successfully escape when |E|<0.5 and r<0.5. However, its escape energy is insufficient, so the Harris hawks surround the rabbit in a hard encirclement before making a surprise pounce. In this phase, they continue to employ two techniques to update their positions. Figure 7 illustrates the mathematical depiction of different Phases of HHO.

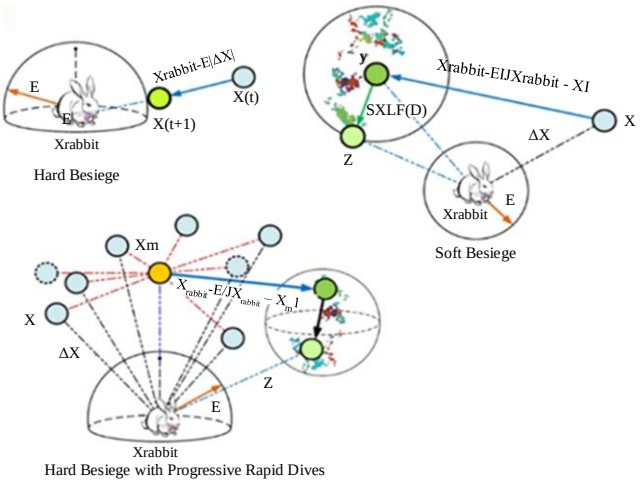

Fig. 7 Mathematical depiction of different phases of HHO

The first technique is,

$$Y = X_{rabbit}(t) - E|JX_{rabbit}(t) - X_m(t)| \quad (23)$$

The second technique is,

$$Z = Y + S * LF(D) \quad (24)$$

For this phase, the updating method can finally be formulated as in Equation (14).

$$X(t+1) = \begin{cases} Y, F(Y) < F\left(X(t)\right) \\ Z, F(Z) < F\left(X(t)\right) \end{cases} \quad (25)$$

3.5. Modified HHO

Two fundamental elements of metaheuristic optimization algorithms are exploration and exploitation, which frequently have opposing goals. Enhancing the efficiency of the traditional HHO algorithm is the objective of the Modified Harris Hawks Optimizer (MHHO). While HHO operates in two stages exploration and exploitation MHHO primarily

focuses on enhancing the latter. This stage focuses on local search near viable solutions to enhance optimization results. In order to accomplish this, the exploitation phase incorporates the sine-cosine approach, which is well-known for its capacity to provide a variety of solutions and oscillate towards optimal solutions [26]. Equation (26) illustrates the improved equation that results from integrating the sine-cosine function into Equations (15) and (18).

$$X(t+1) = X(t) + r_1 cos(r_2)|X_{rabbit}(t) - X(t)| \quad (26)$$

Where rand is a random integer that changes with each iteration, and $r_2 = 2 * \pi * rand(0,1)$.

Equation (27) is the modified version of Hard Besiege Equation (18).

$$X(t+1) = X(t) + r_1 sin(r_2)|X_{rabbit}(t) - X(t)| \quad (27)$$

The overall steps of the MHHO technique in the proposed study are depicted in Figure 8.

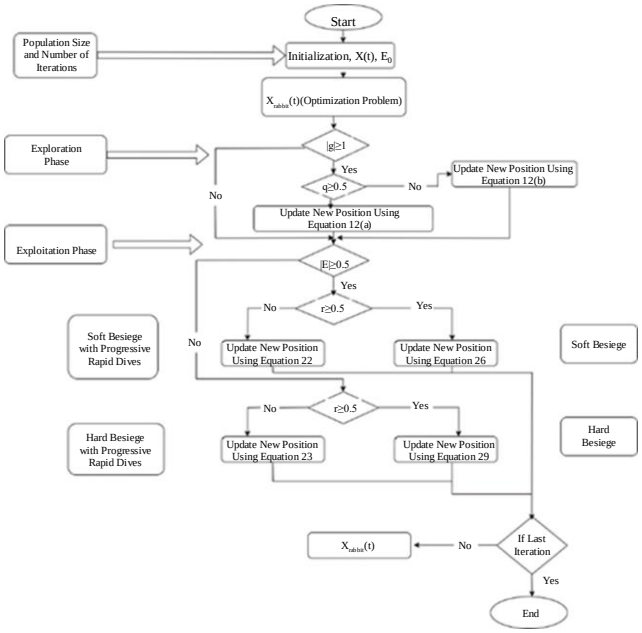

Fig. 8 Flowchart of proposed MHHO

MHHO's computational complexity is still comparable to that of HHO. This involves the complicated nature of the initiation, fitness assessment, and updating procedures. Given a problem dimension of D, T iterations, and a population size of N hawks, the computing load for MHHO is the same as that of HHO. As a result, there are no differences between MHHO and HHO in terms of the complexity of starting the algorithm, determining fitness for each iteration, and updating hawk positions during the optimization process. Its consistency in computational complexity guarantees that MHHO performs as well and scales up to match the efficiency of its predecessor, even with different issue sizes and levels of complexity.

Initialization Complexity: O(N)

Fitness Evaluation Complexity: O(T*N)

Updating Complexity: O(T*N*D)

Total Complexity of MHO: O(N*(T+TD+1))

3.6. Hybrid SVR Algorithm

Precisely determining the model parameters of SVR, notably c, γ, and ε, is critical to optimize SVR performance. However, the wide range of these factors makes it difficult to choose the best values, creating a wide search space. This selection procedure requires effectively applying optimization tools to solve it as an optimization issue. This study created two hybrid models, SVR-MHHO and SVR-PSO, by integrating SVR with nature-inspired algorithms, including PSO and MHHO. These hybrid models improve the efficacy of the SVR model by using MHHO and PSO to calculate the SVR parameters. Figure 9 shows the development process of these hybrid models.

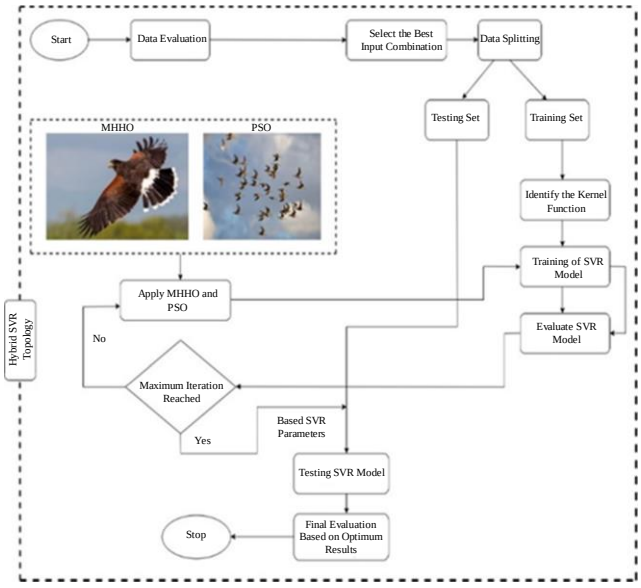

Fig. 9 Flowchart of proposed hybrid SVR Models

3.7. Performance Evaluation

The following performance evaluation criteria were used to evaluate the suggested algorithms and the conventional SVR models thoroughly.

$$R^2 = 1 - \frac{\sum_{1=1}^{N}[O_{obsi} - O_{comi}]^2}{\sum_{i=1}^{N}[O_{obsi} - \bar{O}_{obsi}]^2} \quad (28)$$

$$RMSE = \sqrt{\frac{\sum_{i=1}^{N}(O_{obsi} - O_{comi})^2}{N}} \quad (29)$$

$$R = \frac{\sum_{i=1}^{N}(O_{obsi}-\bar{O}_{obsi})(O_{comi}-\bar{O}_{comi})}{\sqrt{\sum_{i=1}^{N}(O_{obsi}-\bar{O}_{obsi})^2 \sum_{i=1}^{N}(O_{comi}-\bar{O}_{comi})^2}} \quad (30)$$

$$MSE = \frac{1}{N}\sum_{I=1}^{N}(O_{obsi} - O_{comi})^2 \quad (31)$$

$$MAPE = \frac{1}{N}\left[\sum_{i=1}^{N}\left|\frac{O_{obsi}-O_{comi}}{O_{obsi}}\right|\right] \quad (32)$$

The degree of agreement between observed and predicted values is indicated by the coeefficient of determination (R^2), where larger values correspond to better prediction accuracy. R^2 has a range of -1 to 1, with values closer to 1 denoting stronger agreement. In the meantime, the degree of association among the simulated and predicted data points is revealed by the correlation coefficient (R).

Calculated by dividing absolute errors by the total number of observations, MSE, RMSE, and MAPE are measures of relative errors. These metrics are essential for evaluating predictive models in various industries since they provide useful data regarding prediction accuracy. Because Mean Absolute Error (MAPE) is scale-independent, it is very beneficial when comparing the performance of forecasts across various datasets. Another popular statistical metric, Root Mean Square Error (RMSE), is employed to compare prediction errors across various approaches; smaller readings correspond to superior prediction accuracy. These five statistical factors were thoroughly evaluated in this study to identify the best predictive model, which resulted in extremely accurate predictions.

4. Results and Discussion

Using a multi-city strategy, the main goal of this study is to develop hybrid SVR techniques (SVR-MHHO and SVR-PSO) and evaluate how well they predicted fluctuations in load demand across remote locations in the Indian cities of Delhi, Mumbai, Kolkata and Bangalore. In order to accomplish this, information regarding the load profiles of residential blocks each with ten apartments was gathered via surveys carried out in the corresponding cities. Each apartment's specifics, including the quantity of electrical appliances, ratings, and usage patterns, were carefully documented. Physical monitoring was then used to get hourly load data, recording unrestrained load fluctuations throughout 24 hours. A bar plot of the data gathered from the four isolated locations is depicted in Figure 10.

The correlation matrix shown in Figure 11 reveals that among the variables considered, ambient temperature exhibits the strongest correlation with the target value in Delhi, Mumbai, and Kolkata, followed by wind speed and solar radiation. However, wind speed emerges as the most influential variable in Bangalore, followed by ambient temperature and solar radiation. Specifically, temperature demonstrates a strong correlation across all cities, with coefficients of 0.95, 0.93, 0.92, and 0.88 for Bangalore, Kolkata, Delhi, and Mumbai, respectively. Wind speed also exhibits noteworthy correlations, ranging from 0.63 to 0.72 across the four cities. Conversely, solar radiation demonstrates only marginal to fair correlations, with coefficients ranging from -0.15 to 0.24 for Delhi, Mumbai, Kolkata, and Bangalore, respectively.

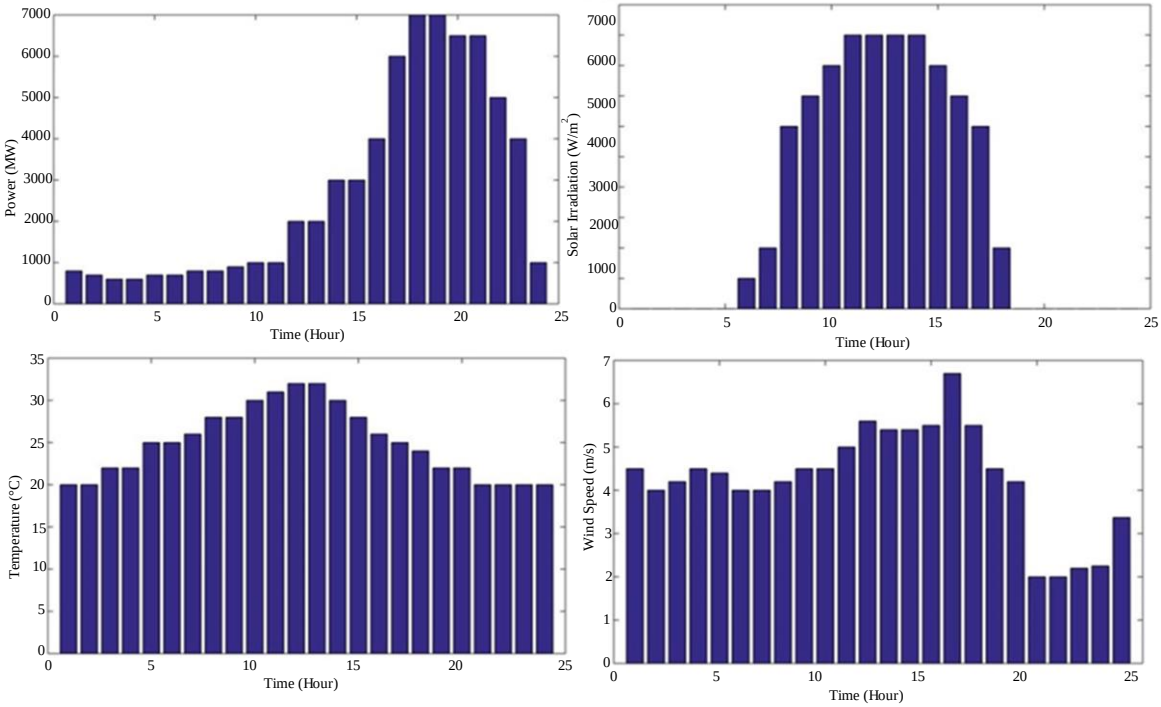

(a) Delhi

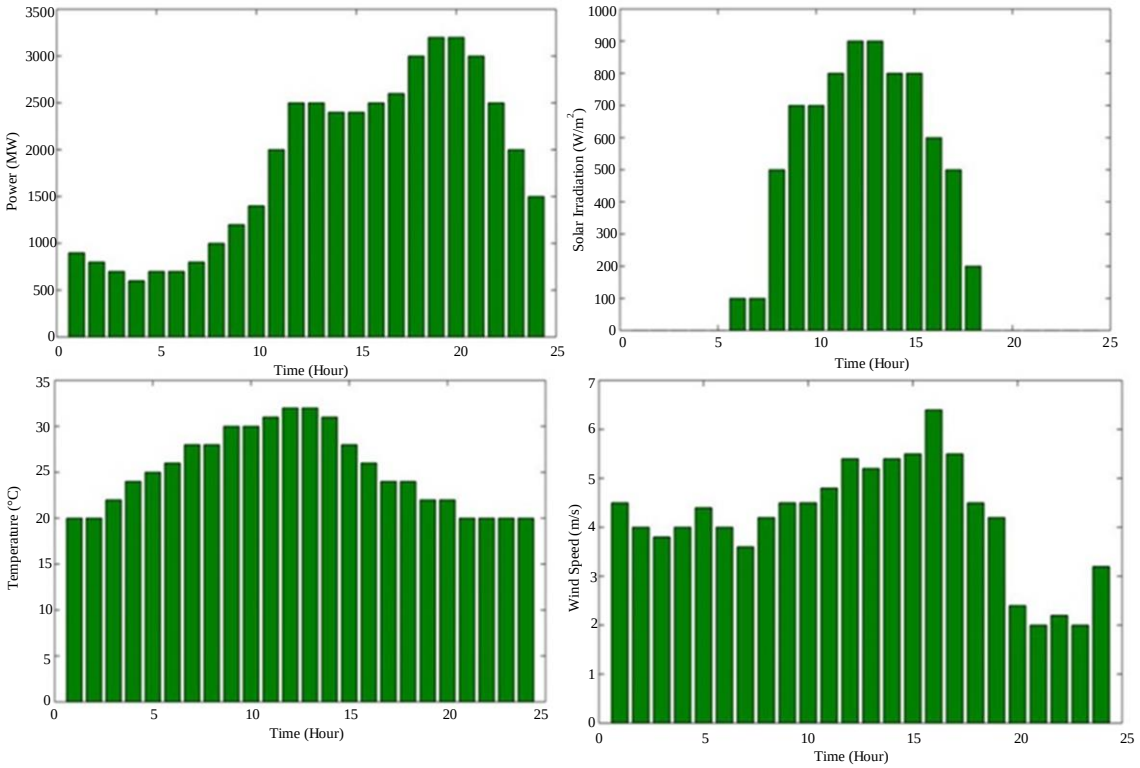

(b) Mumbai

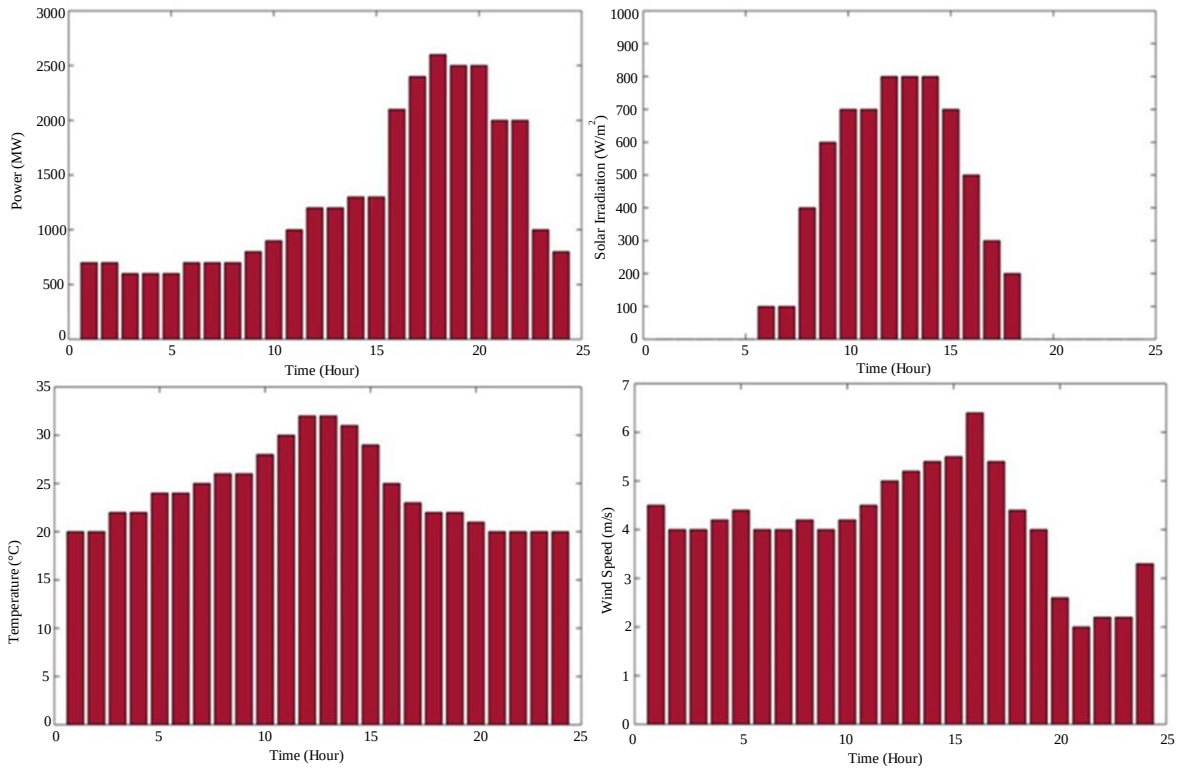

(c) Kolkata

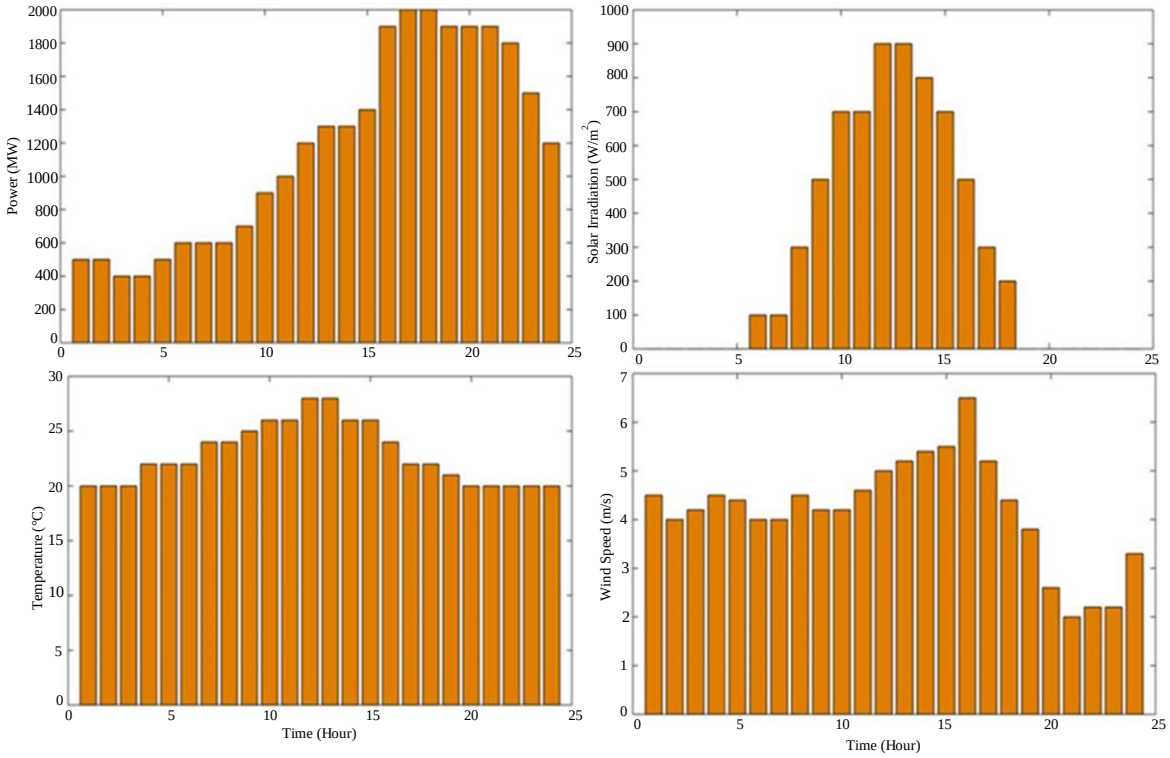

(d) Bangalore

Fig. 10 Bar plot displaying the raw data for selected cities

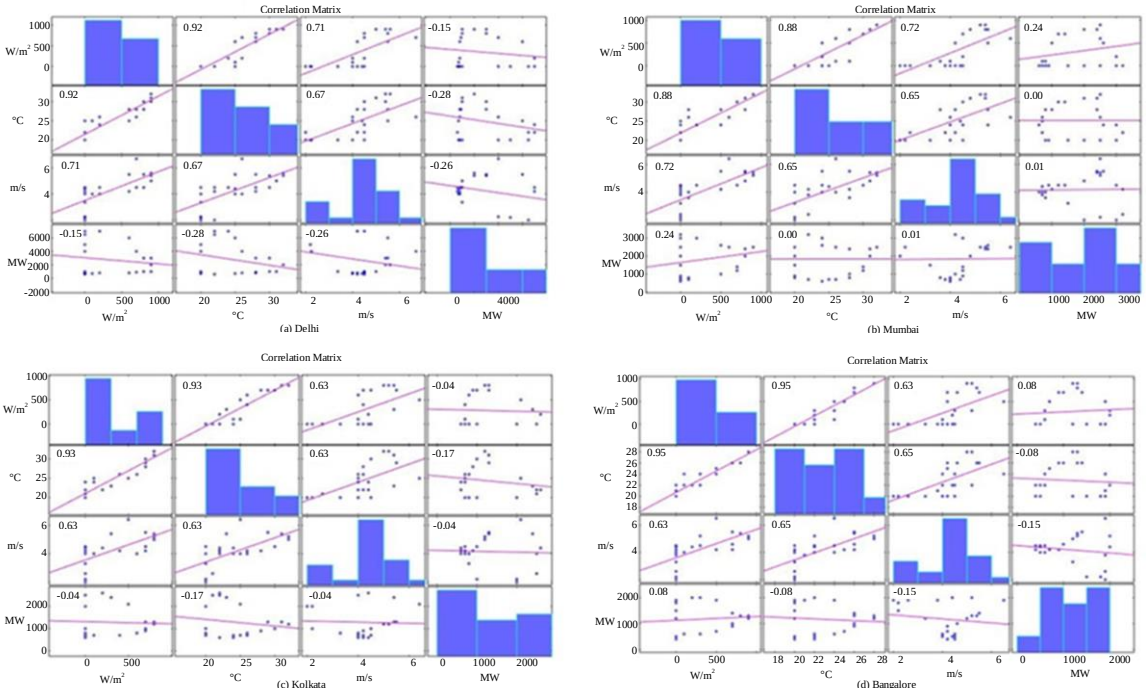

Fig. 11 Correlation matrices of the variables for selected cities

The most popular performance metrics, such as R^2, MSE, RMSE, R and MAPE for both calibration and verification were used to assess the model simulation. Table 1 presents the simulated outcomes of quantitative assessment based on modeling combinations according to Equation (2).

Table 1. Evaluation outcomes for conventional SVR models

Phase	Cities	Models	R+	MSE	RMSE	R	MAPE
Calibration	Delhi	SVR-M1	0.6752	0.0165	0.1285	0.8254	1.7853
		SVR-M2	0.9217	0.0038	0.0616	0.9592	0.8372
		SVR-M3	0.9645	0.0019	0.0436	0.9794	0.6758
	Mumbai	SVR-M1	0.4478	0.0372	0.1929	0.6701	3.3862
		SVR-M2	0.4671	0.0358	0.1892	0.6814	4.2123
		SVR-M3	0.7856	0.0158	0.1256	0.8983	1.5432
	Kolkata	SVR-M1	0.8021	0.0095	0.0975	0.9078	1.8056
		SVR-M2	0.6183	0.0169	0.1301	0.7894	0.7023
		SVR-M3	0.9774	0.0008	0.0283	0.9912	1.0321
	Bangalore	SVR-M1	0.6043	0.0423	0.2057	0.7765	2.0231
		SVR-M2	0.7174	0.0308	0.1756	0.8397	2.0456
		SVR-M3	0.7216	0.0304	0.1748	0.8412	2.6137
Verification	Delhi	SVR-M1	0.6938	0.0152	0.1233	0.8337	1.7524
		SVR-M2	0.9153	0.0042	0.0648	0.9556	0.8231
		SVR-M3	0.9683	0.0015	0.0387	0.9827	0.6923
	Mumbai	SVR-M1	0.4326	0.0392	0.1980	0.6548	3.4721
		SVR-M2	0.4497	0.0376	0.1940	0.6672	4.3142
		SVR-M3	0.7982	0.0146	0.1209	0.8836	1.5867
	Kolkata	SVR-M1	0.8167	0.0084	0.0917	0.9042	1.8754
		SVR-M2	0.6387	0.0162	0.1273	0.7995	0.7212
		SVR-M3	0.9805	0.0007	0.0267	0.9932	1.0054
	Bangalore	SVR-M1	0.6128	0.0415	0.2037	0.7803	2.1567
		SVR-M2	0.7239	0.0295	0.1717	0.8497	2.1893
		SVR-M3	0.7281	0.0291	0.1706	0.8531	2.7341

The multi-city effectiveness of the approach depending on various input variables is also shown in Table 1 for both the calibration and verification phases. Based on the evaluation criteria, it is evident from the results that the predictive modeling methodologies yielded varying levels of adequacy. Furthermore, the total multi-city findings show that, in terms of R^2, $MSE, RMSE, R$, and $MAPE$, SVR-M3 was the best simulation. While ranking the models based on the attained accuracies is challenging, the SVR-M3 strategy demonstrated the best prediction accuracy, with Delhi and Kolkata achieving over 95% and Mumbai exceeding 78% in terms of goodness of fit.

R2 and R reveal the degree of association between simulated and predicted data points among the performance evaluation parameters prediction accuracy. The relative errors are measured using the parameters MSE, RMSE and MAPE. Error values needed to be small, and R2 values needed near 1 for better prediction accuracy. Here, by observing both the calibration and verification data sets from Table 1, it is found that the SVR-M3 model shows a relatively small error percentage and better prediction accuracy for all the major cities taken here. So, the SVR-M3 is the best model among all three models taken.SVR-M3 shows the best prediction accuracy, with more than 96% for Delhi and Kolkata. In the verification phase, Mumbai displayed 79%, and Bangalore displayed more than 72% goodness of fit.

The proposed three models are compared across multiple cities in the scatter plots shown in Figure 12. These plots provide insights into the overall goodness of fit by visually representing the agreement between the observed and expected loads. It is clear from observation that the $SVR - M3$ model is more accurate than the $SVR - M1$ and $SVR - M2$ models. This suggests that $SVR - M3$ predicts values that are relatively close to the observed load values in all cities that are considered.

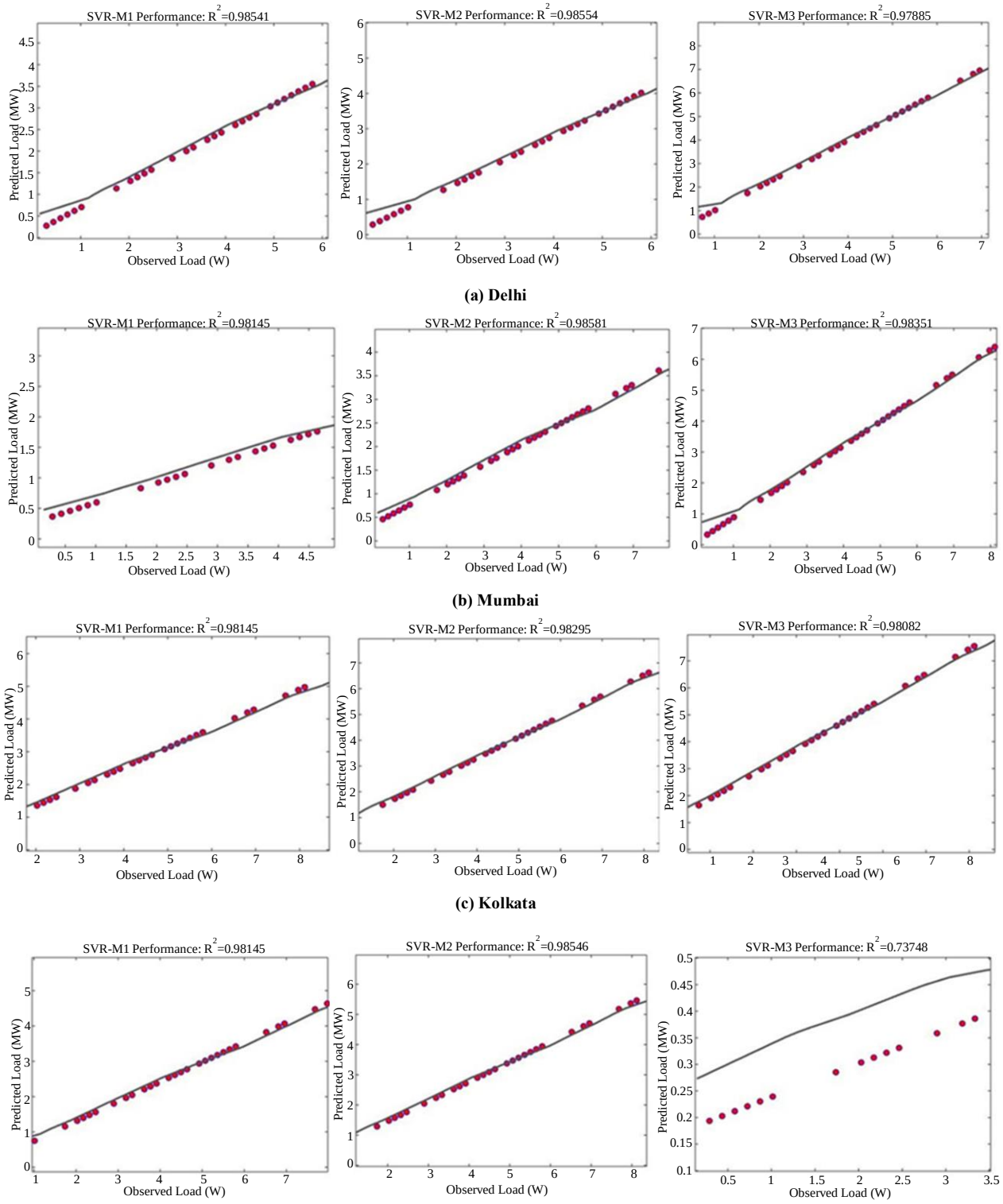

Fig. 12 Scatter Plots of SVR

To assess the load demand prediction, a dimensional radar diagram, as shown in Figure 13, can be used for an extra perceptive analysis. The figure illustrates that $SVR-M3$ performs better than the other SVR models, with $SVR-M2$ and $SVR-M1$ coming in second and third, respectively. In particular, SVR-M3 regularly performs better than the other

models in capturing the fitting pattern in Bangalore ($R^2 > 0.73$), Mumbai ($R^2 > 0.9$), and Delhi ($R^2 > 0.9$). In Kolkata, on the other hand, the model's effectiveness is ranked as follows: $SVR - M3 > SVR - M1 > SVR - M2$, and its R^2 value is an astounding 0.97. This very informative image shows how different SVR models perform differently in different regions in terms of predicted accuracy.

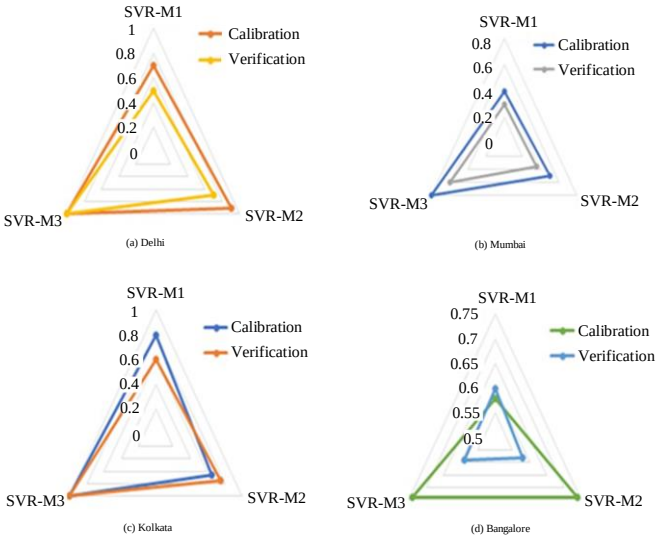

Fig. 13 Radar graph

Temperature, wind, and sun radiation are the three main variables that SVR-M3 uses in its prediction method, which accounts for its remarkable success. Improved predictive capabilities are demonstrated by $SVR - M3$, which incorporates all pertinent criteria that have a major impact on load demand prediction. $SVR - M3$ also performs better than $SVR - M1$ and $SVR - M2$ in terms of MSE according to the quantitative evaluation conducted across several cities. $SVR - M3$ has better predictive accuracy than $SVR - M1$ and $SVR - M2$, as seen by its lower MSE value of 0.0015 as opposed to 0.0152 and 0.0042, respectively.

Despite attempts to consider the non-linear relationship among predictors and their related objectives, Mumbai's prediction accuracy was still far from ideal, with many errors and ambiguity. In order to tackle this problem, including optimization techniques like PSO and MHHO could enhance forecasting accuracy and lessen the noted difficulties. Although promising estimations are made in the calibration phase which concentrates on fine-tuning models using known targets and input variables the testing phase is critical to evaluate a model's accuracy with unknown target values. Unlike the training set, this stage offers an advantageous possibility to confirm the model's dependability. Table 2 provides an overview of the efficacy of SVR-PSO and SVR-MHHO by displaying the findings for both the training and verification stages.

Table 2. Findings from SVR-PSO and SVR-MHHO

Phase	Cities	Models	R^2	MSE	RMSE	R	MAPE
Calibration	Delhi	SVR-PSO	0.9702	0.0017	0.0412	0.9843	0.3826
	Mumbai		0.8245	0.0123	0.1109	0.9076	0.1554
	Kolkata		0.9781	0.0011	0.0329	0.9892	0.1987
	Bangalore		0.8657	0.0145	0.1204	0.9298	0.2125
	Delhi	SVR-MHHO	0.9932	0.0004	0.0200	0.9961	0.1479
	Mumbai		0.8896	0.0062	0.0787	0.9423	0.1323
	Kolkata		0.9921	0.0005	0.0224	0.9952	0.0768
	Bangalore		0.9287	0.0078	0.0884	0.9624	0.1896
Verification	Delhi	SVR-PSO	0.9592	0.0053	0.0728	0.9786	0.4213
	Mumbai		0.7045	0.0271	0.1646	0.8321	0.1967
	Kolkata		0.9573	0.0055	0.0742	0.9781	0.2324
	Bangalore		0.7189	0.0318	0.1782	0.8446	0.2435
	Delhi	SVR-MHHO	0.9852	0.0013	0.0359	0.9913	0.1726
	Mumbai		0.9714	0.0021	0.0458	0.9856	0.1852
	Kolkata		0.9776	0.0017	0.0412	0.9892	0.0945
	Bangalore		0.8997	0.0098	0.0990	0.9492	0.2223

According to the findings presented in Table 2, SVR-MHHO exhibits superior performance across all evaluated metrics for the regions of Delhi, Mumbai, Kolkata, and Bangalore. With R^2 values of 0.9932, 0.8896, 0.9921, and 0.9287 correspondingly, SVR-MHHO notably obtains the highest values. Its accuracy in anticipating load demand

variability is further demonstrated by the smaller MSE values of 0.0004, 0.0062, 0.0005, and 0.0078. The smaller MAPE values are also produced by SVR-MHHO, which registers 0.1479, 0.1323, 0.0768, and 0.1896 for the same locations. Based on these findings, it is clear that SVR-MHHO is a better model than SVR-PSO for accurately modeling load demand in the Delhi, Mumbai, Kolkata, and Bangalore regions. Examining the boxplots shown in Figure 14 further emphasizes the exploratory study of the SVR-PSO and SVR-MHHO approaches. The boxplots illustrate how well the calculated models captured the patterns of observed values. The most effective models closely match the observed values determined by the box and whisker evolution criterion. After analysis, the SVR-MHHO framework performs better than the SVR-PSO and SVR-M3 approaches, showing better degree and trend patterns among the computed and measured values. As a result, the SVR-MHHO model is ranked highest out of all the models examined.

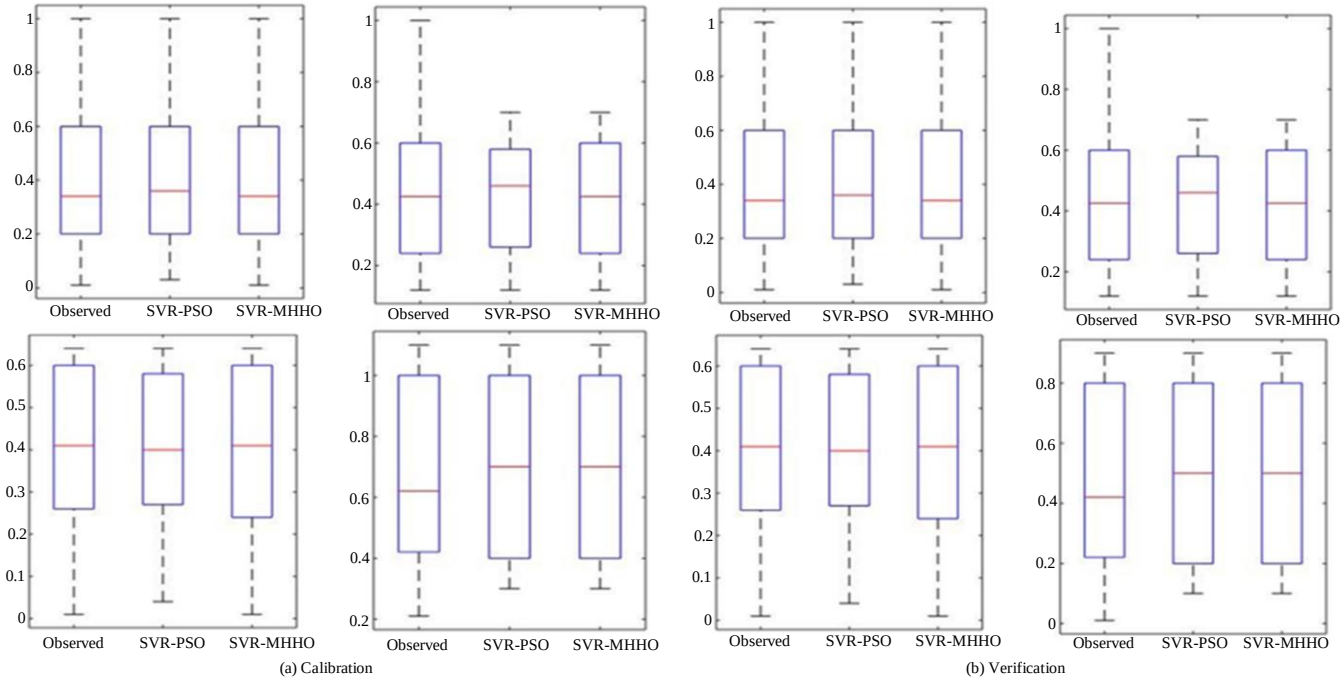

Fig. 14 Boxplot for SVR-PSO and SVR-MHHO models

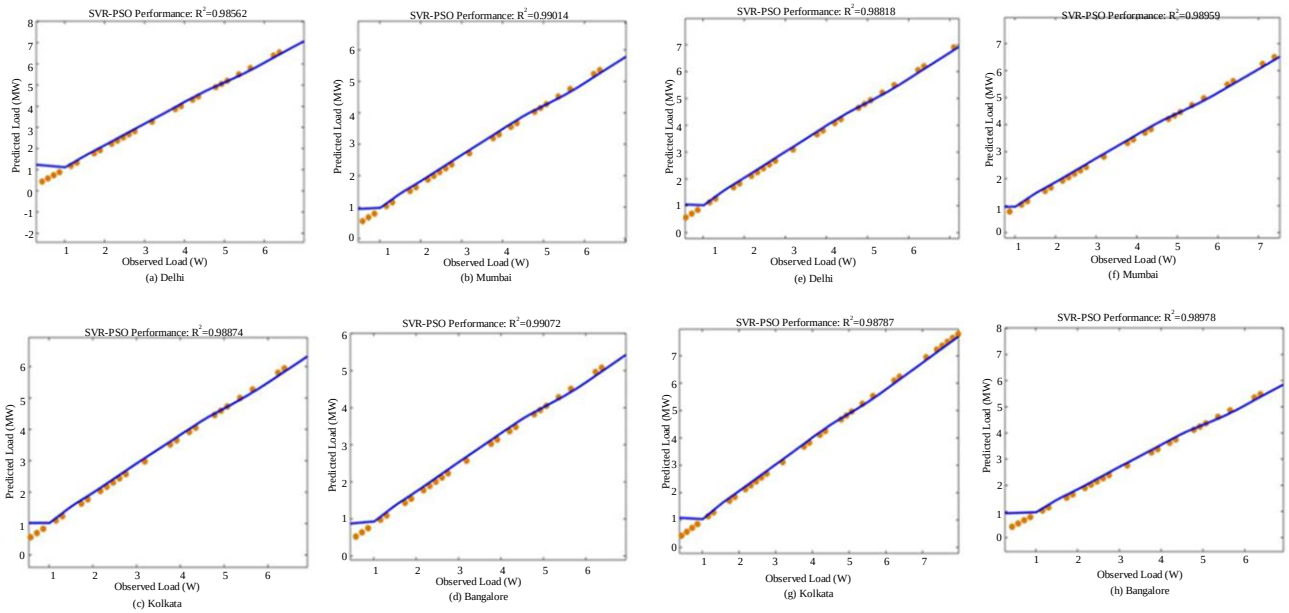

Fig. 15 Scatter plot for SVR-PSO and SVR-MHHO

The relationship between the actual and forecasted values for SVR-PSO and SVR-MHHO in Delhi, Mumbai, Kolkata, and Bangalore is shown by the scatter plots in Figure 15. Compared to SVR-PSO, SVR-MHHO notably shows a better correlation between observed and predicted values. All of the models' R values are also greater than 0.9, consistent with the general agreement that R values greater than 0.70 are appropriate. Therefore, it is determined that all optimization method models produce satisfactory outcomes. Time series graphs in Figure 16 provide a more effective way to visualize the simulated findings. The SVR-MHHO algorithm outperforms SVR alone in terms of reliability, reliably producing the optimal anticipated load across all four cities. Although there are several major metaheuristic algorithms, neither can ensure consistently excellent results across varied issue types. Nonetheless, current studies on the innovative population-based, nature-inspired optimization paradigm (MHHO) model have successfully identified the best answers for multi- and higher-dimensional issues. This innovative optimizer was thoroughly assessed using comparisons with other nature-inspired methods on 29 benchmark tasks and other real-world engineering applications.

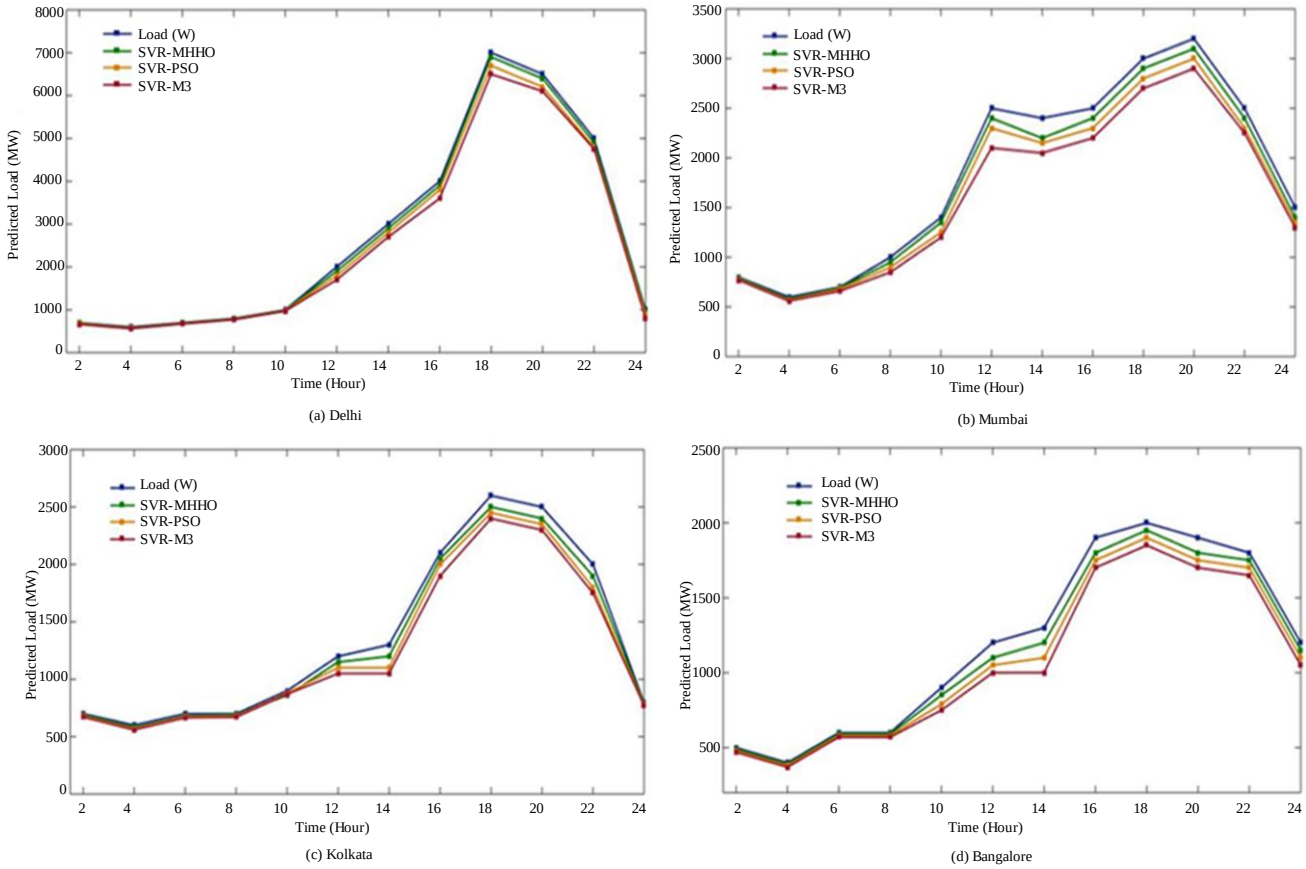

Fig. 16 Every data index's time series graph

5. Conclusion

The study highlighted the impact of population density and weather conditions on demand fluctuation and addressed the significance of load demand forecasts in energy management and infrastructure design. Despite being widely employed, conventional SVR models had difficulty capturing complicated interactions, especially in areas with non-linear consumption patterns. SVR-MHHO and SVR-PSO, two hybrid SVR algorithms that use metaheuristic optimization approaches, were developed to address these problems. Through integrating PSO and MHHO, these algorithms sought to improve predicted accuracy and optimize the parameters of the SVR model.

Extensive testing revealed that SVR-MHHO and SVR-PSO outperformed conventional SVR models in terms of performance, demonstrating their capacity to forecast load demand fluctuation in various geographical areas reliably. The best conventional SVR model, according to sensitivity analysis of input attribute values, is SVR-M3. All cities showed substantial improvements in performance for the hybrid SVR algorithms, particularly SVR-MHHO, with lower MSE and MAPE values and higher R^2 values.

These results demonstrated the ability of SVR-MHHO and SVR-PSO to forecast load demand fluctuation precisely, which could assist with infrastructure development and energy

management initiatives. Overall, the study laid the groundwork for more accurate and reliable load demand forecasting, offering valuable insights for energy management initiatives in various geographical contexts. By addressing the limitations of conventional SVR models and leveraging advanced optimization techniques, the proposed hybrid SVR algorithms pave the way for enhanced energy management strategies and sustainable development in the future. Future research can focus on incorporating real-time data from IoT-enabled smart grids and energy monitoring systems to enhance hybrid SVR models' adaptability and accuracy in dynamic environments. Also, the use of multi-objective optimization techniques to balance competing goals, such as minimizing energy waste, reducing operational costs, and optimizing grid reliability, will be explored.

Acknowledgments

The author profoundly appreciates the supervisor's guidance and unwavering support throughout this study.

References

[1] Mohamed I. Ibrahem, "*Privacy-Preserving and Efficient Electricity Theft Detection and Data Collection for AMI Using Machine Learning*," Doctoral Dissertation, Tennessee Technological University, 2021. [Google Scholar]

[2] Yanbing Lin et al., "An Ensemble Model Based on Machine Learning Methods and Data Preprocessing for Short-Term Electric Load Forecasting," *Energies*, vol. 10, no. 8, 2017. [CrossRef] [Google Scholar] [Publisher Link]

[3] Gamze Nalcaci, Ayse Özmen, and Gerhard Wilhelm Weber, "Long-Term Load Forecasting: Models Based on MARS, ANN and LR Methods," *Central European Journal of Operations Research*, vol. 27, pp. 1033-1049, 2019. [CrossRef] [Google Scholar] [Publisher Link]

[4] O. Demirel, A. Kakilli, and M. Tektas, "Electric Energy Load Forecasting Using ANFIS and ARMA Methods," *Journal of the Faculty of Engineering and Architecture of Gazi University*, vol. 25, no. 3, pp. 601-610, 2010. [Google Scholar] [Publisher Link]

[5] Jiarui Zhang, "Research on Power Load Forecasting Based on the Improved Elman Neural Network," *Chemical Engineering Transactions*, vol. 51, pp. 589-594, 2016. [CrossRef] [Google Scholar] [Publisher Link]

[6] Eisa Almeshaiei, and Hassan Soltan, "A Methodology for Electric Power Load Forecasting," *Alexandria Engineering Journal*, vol. 50, no. 2, pp. 137-144, 2011. [CrossRef] [Google Scholar] [Publisher Link]

[7] Sheraz Aslam et al., "A Survey on Deep Learning Methods for Power Load and Renewable Energy Forecasting in Smart Microgrids," *Renewable and Sustainable Energy Reviews*, vol. 144, 2021. [CrossRef] [Google Scholar] [Publisher Link]

[8] Xavier Serrano-Guerrero et al., "A New Interval Prediction Methodology for Short-Term Electric Load Forecasting Based on Pattern Recognition," *Applied Energy*, vol. 297, 2021. [CrossRef] [Google Scholar] [Publisher Link]

[9] Mahmoud M. Badr et al., "Privacy-Preserving Federated-Learning-Based Net-Energy Forecasting," *SoutheastCon 2022*, pp. 133-139, 2022. [CrossRef] [Google Scholar] [Publisher Link]

[10] Chafak Tarmanini et al., "Short Term Load Forecasting Based on ARIMA and ANN Approaches," *Energy Reports*, vol. 9, pp. 550-557, 2023. [CrossRef] [Google Scholar] [Publisher Link]

[11] Nooriya A. Mohammed, and Ammar Al-Bazi, "An Adaptive Backpropagation Algorithm for Long-Term Electricity Load Forecasting," *Neural Computing and Applications*, vol. 34, no. 1, pp. 477-491, 2022. [CrossRef] [Google Scholar] [Publisher Link]

[12] Badar ul Islam, and Shams Forruque Ahmed, "Short-Term Electrical Load Demand Forecasting Based on LSTM and RNN Deep Neural Networks," *Mathematical Problems in Engineering*, 2022. [CrossRef] [Google Scholar] [Publisher Link]

[13] Majed A. Alotaibi, "Machine Learning Approach for Short-Term Load Forecasting Using Deep Neural Network," *Energies*, vol. 15, no. 17, 2022. [CrossRef] [Google Scholar] [Publisher Link]

[14] Sivakavi Naga Venkata Bramareswara Rao et al., "Day-Ahead Load Demand Forecasting in Urban Community Cluster Microgrids Using Machine Learning Methods," *Energies*, vol. 15, no. 17, 2022. [CrossRef] [Google Scholar] [Publisher Link]

[15] Eduardo Machado et al., "Electrical Load Demand Forecasting Using Feed-Forward Neural Networks," *Energies*, vol. 14, no. 22, 2021. [CrossRef] [Google Scholar] [Publisher Link]

[16] Seyed Mohammad Jafar Jalali et al., "A Novel Evolutionary-Based Deep Convolutional Neural Network Model for Intelligent Load Forecasting," *IEEE Transactions on Industrial Informatics*, vol. 17, no. 12, pp. 8243-8253, 2021. [CrossRef] [Google Scholar] [Publisher Link]

[17] Arash Moradzadeh et al., "A Secure Federated Deep Learning-Based Approach for Heating Load Demand Forecasting in Building Environment," *IEEE Access*, vol. 10, pp. 5037-5050, 2021. [CrossRef] [Google Scholar] [Publisher Link]

[18] Shafiul Hasan Rafi et al., "A Short-Term Load Forecasting Method Using Integrated CNN and LSTM Network," *IEEE Access*, vol. 9, pp. 32436-32448, 2021. [CrossRef] [Google Scholar] [Publisher Link]

[19] Lulu Wen, Kaile Zhou, and Shanlin Yang, "Load Demand Forecasting of Residential Buildings Using a Deep Learning Model," *Electric Power Systems Research*, vol. 179, 2020. [CrossRef] [Google Scholar] [Publisher Link]

[20] Ghulam Hafeez, Khurram Saleem Alimgeer, and Imran Khan, "Electric Load Forecasting Based on Deep Learning and Optimized by Heuristic Algorithm in Smart Grid," *Applied Energy*, vol. 269, 2020. [CrossRef] [Google Scholar] [Publisher Link]

[21] Vladimir N. Vapnik, *The Nature of Statistical Learning Theory*, 2nd ed., Springer Science & Business Media, Springer New York, 2000. [CrossRef] [Google Scholar] [Publisher Link]

[22] D. Han, L. Chan, and N. Zhu, "Flood Forecasting Using Support Vector Machines," *Journal of hydroinformatics*, vol. 9, no. 4, pp. 267-276, 2007. [CrossRef] [Google Scholar] [Publisher Link]

[23] J. Kennedy, and R. Eberhart, "Particle Swarm Optimization," *Proceedings of the ICNN'95 - International Conference on Neural Networks*, Perth, Australia, pp. 1942-1948, 1995. [CrossRef] [Google Scholar] [Publisher Link]

[24] Ali Asghar Heidari et al., "Harris Hawk's Optimization: Algorithm and Applications," *Future Generation Computer Systems*, vol. 97, pp. 849-872, 2019. [CrossRef] [Google Scholar] [Publisher Link]

[25] Dieu Tien Bui et al., "A Novel Swarm Intelligence Technique for Spatial Assessment of Landslide Susceptibility," *Sensors*, vol. 19, no. 16, 2019. [CrossRef] [Google Scholar] [Publisher Link]

[26] Abdelhady Ramadan et al., "Photovoltaic Cells Parameter Estimation Using an Enhanced Teaching-Learning-Based Optimization Algorithm," *Iranian Journal of Science and Technology, Transactions of Electrical Engineering*, vol. 44, pp. 767-779, 2020. [CrossRef] [Google Scholar] [Publisher Link]